IEEE Access
Multidisciplinary ⋮ Rapid Review ⋮ Open Access Journal

Received November 2, 2019, accepted November 25, 2019, date of publication December 9, 2019,
date of current version December 23, 2019.

Digital Object Identifier 10.1109/ACCESS.2019.2958415

Weighting Factors Optimization of Model Predictive Torque Control of Induction Motor Using NSGA-II With TOPSIS Decision Making

M. H. ARSHAD[1], (Student Member, IEEE), M. A. ABIDO[1,2], (Senior Member, IEEE), ABOUBAKR SALEM[1], (Member, IEEE), AND ABUBAKR H. ELSAYED[1]
[1]Department of Electrical Engineering, King Fahd University of Petroleum and Minerals, Dhahran 31261, Saudi Arabia
[2]King Abdullah City for Atomic and Renewable Energy (K.A.CARE), Dhahran 31261, Saudi Arabia

Corresponding author: M. A. Abido (mabido@kfupm.edu.sa)

This work was supported in part by the Deanship of Scientific Research of the King Fahd University of Petroleum and Minerals through the Electrical Power & Energy Systems Research Group under Project RG171002, and in part by the King Abdullah City for Atomic and Renewable Energy (K. A. CARE).

ABSTRACT Model predictive control (MPC) is the result of the latest advances in power electronics and modem control. It is regarded as one of the best techniques when it comes to handling of nonlinearities in the intrinsic model of induction motor (IM). Conventional MPC utilizes weighting factors in the objective function that are tuned after rigorous experimental work which can be improved by utilizing the more mature intelligent optimization techniques like NSGA-II etc. In this study, the weighting factor optimization for the conventional MPC control of IM based on NSGA-II with TOPSIS decision-making criteria is studied. A control algorithm is designed, and an experimental test setup is made to obtain the results of this intelligent MPC which are compared with conventional MPC based on some performance indices like torque and flux ripple, switching frequency loss etc.

INDEX TERMS DTC, dynamic induction motor model, FOC, finite set control model non-dominated sorting genetic algorithm, predictive control, TOPSIS.

I. INTRODUCTION

The fundamental difference of electrical drive systems to mechanical systems is the ease of control, their spontaneous startup and fully-loaded with a simple command from even a remote location. During the last few decades, developments in the fields of power electronics, electric machines, and control theories have made AC drives more viable and inexpensive when compared in terms of drive overall performance and cost to DC drives [1]. Among various types of AC machines, the asynchronous machine (also called induction motor) is the most used machine in industry, it is more robust, reliable, efficient and low cost compared to other machines (DC & synchronous machine) for similar applications. Increasing concerns about the energy crisis, as well as environmental pollution, significantly promote the development of environmentally friendly electric-drive vehicles (EDVs) [2]–[4] and wind energy conversion systems (WECSs) [5], which make the IM more promising. Almost 11% of vehicle-traction motor manufacturers supply IM and about 6% produce both PMSMs and IMs. Under such circumstances, it is required to develop novel control schemes specifically for the IM-based applications to improve performance, enhance reliability,

Typically, the mainstream control schemes for IMs can be categorized in three ways: scalar control, field-oriented control (FOC), and direct torque control (DTC) [6].

Scalar control, also known as v/f control, is the general-purpose AC motor drives control used in industrial applications. In this scheme, the speed of AC machine is regulated by adjusting the magnitude versus frequency ratio of the stator voltage vector (VV) to maintain the rated air-gap flux of the electric machine. Three-phase reference voltage is converted to inverter gate signals by using a modulator. This control law is based on the steady-state machine model that results in poor transient behavior of the drive also because of the absence of feedback loop the direct electromagnetic-torque control becomes impossible. However, there is no denying that scalar control has several

The associate editor coordinating the review of this manuscript and approving it for publication was Diego Oliva.

advantages, such as simple implementation, low cost, and sensor-less motion. In addition, IM drives with scalar control produces satisfactory steady state response, making them suitable for low power rating applications, such as pumps and fans.

Before FOC (also named vector control or decoupled-current control) was developed, motor control engineers had been plagued by a problem for years: Is it possible to control an AC machine like a DC machine, i.e., can the electromagnetic torque and excitation flux be decoupled and controlled, respectively? This problem was not addressed until field-oriented control was proposed in the late 1970s. It has been reported in literature that the way torque is produced in both AC and DC motor is rather similar [1]. The basic principle of the FOC is to converter the three-phase currents of an AC machine, by using Park transformation, to the orthogonal decoupled components of current corresponding to torque and flux allowing the independent control of field-magnetizing flux or the dynamic response of torque [7]. Following this control scheme, the dynamic response of the electromagnetic torque of AC machines is as fast and precise as that of separately excited DC machines [6]. With the rotor speed information, the FOC motor drive system achieves accurate speed control with good dynamic response. However, compared with scalar control and DTC, the FOC is much more complicated; and accurate position feedback is required.

DTC was initially proposed by a German engineer, Depenbrock [8], and two Japanese scholars, Takahashi and Noguchi [9], in the 1980s. Even though DTC was proposed after FOC, it is regarded as the most ground-breaking control scheme for AC drives also an able substitute for FOC [10]. Contrary to FOC, DTC selects stator flux and electromagnetic torque as two decoupled control parameters to control respective quantities directly without controlling the middlemen, e.g., the armature currents. The advantages of DTC are simple implementation, fast dynamic torque response and invariance to disturbances or parametric variations [1]. The dynamic response of electromagnetic-torque for a DTC drive is almost 10 times quicker than other AC drive systems. In conventional DTC, for each control cycle, an appropriate voltage vector is selected from the all intrinsic vectors of the inverter in accordance to the two control outputs of hysteresis controllers (comparators) to generate gate signals for the inverter. This feature leads to the drawbacks of irregular torque and flux pulsations together with additional harmonic losses. Therefore, reducing the torque and flux ripple levels of the conventional DTC system while retaining its intrinsic merits has become a subject of intense research [11].

In contrary to these mainstream control techniques there is a growing more efficient control technique (based on the discrete model of induction motor) known as Model Predictive Control. In this paper, the performance of finite control set model predictive torque control (FCS-MPTC) of three-phase induction motor (TPIM) fed with three leg six switch inverter (B-6 inverter) is studied through simulations. The idea is to optimize the weighting factors for the cost function in the conventional FCS-MPTC for better performance. The proposed technique leads to reduced input phase current, torque and flux ripple also improves the switching frequency losses.

The remainder of this paper is structured as follows: Section II brief literature overview of MPC section III describes the discrete model of the induction motor used for conventional MPC. Section IV briefly introduces the B-6 inverter and its SV control architecture. Section V and VI are dedicated to MPC control and the proposed optimization strategy. The results obtained are discussed in Section VII using tabular and pictorial illustrations. Finally, last section concludes the paper.

II. LITERATURE REVIEW OF MPC

In the literature, there have been a lot of attempts to improve the performance of the IM drive. The major problem with the DTC is the steady state torque ripple. Historically, a great amount of improved DTC techniques has been developed from various perspectives to suppress the ripple levels and lower the demand on the hardware, as well as the sampling rates. The basic idea is to increase the number of available voltage vectors to better correct the errors of torque and stator flux magnitudes. One effective technique for ripple reduction is to use the SVPWM, commonly used in the FOC-based three-phase motor control systems, into the DTC [12]. The investigated SVM-DTC technique in [13], first acquired reference voltage in synchronously rotating frame of reference and then by using inverse park transformation, transformed it into stationary frame of reference, while in [14], direct stationary frame of reference values of voltage reference is used with no stator flux magnitude PI controller. The stator flux is usually estimated in DTC by using pure integrator which results in DC drifts because of non-zero initial flux of the IM, As far as FOC is concerned, a cascaded structure of two control loops, and outer loop for speed and an inner loop for current, is used which limits the use of high switching frequency especially desired for high power drive applications that ultimately reduced the dynamic response of the FOC during speed variations. The precise estimation of the flux in required for FOC. Model reference adaptive system (MARS) and Kalman filter based method has been utilized in [15], [16] for flux estimation which increases the computational complexity of the drive

In [14], the model predictive DTC calculates the future torque states associated with all of the available voltage vectors in the next time interval and then an optimal voltage-vector is chosen based on the outcomes subjected to a performance-oriented objective function. Sliding mode observers (SMO) has best serves the purpose in [17]. Because of the simple implementation and robustness of SMO, it has been widely accepted for flux estimation, but the chattering problem associated with SMO degrades the overall drive performance.

Furthermore, MPC techniques are simple and based on instinctive formulation and are widely used for multi-variable nonlinear systems because of its ability to handle the constraints easily and effectively. Although MPC require large calculation and in the past, it was used solely for the process having a large time constant especially in chemical and process control engineering applications [18], [19], but with the latest advent in power electronics devices along with recent capable micro-processors have made it possible to use MPC in motor drives [20], [21]. The MPC generates, at each sampling moment, a control law from the minimization of a cost function, which takes into account the error between output prediction and future references. Usually in the cost function, terms are added that allows to adjust the effort of control and also improves numerical stability. Another feature that makes MPC attractive is the possibility of explicitly dealing with the restrictions in formulation of control [19]. Several variations of MPC have been reported in the literature for motor drives [22], [23] that can be classified based on optimization methodology, prediction horizon and the cost function as shown in Figure 1.

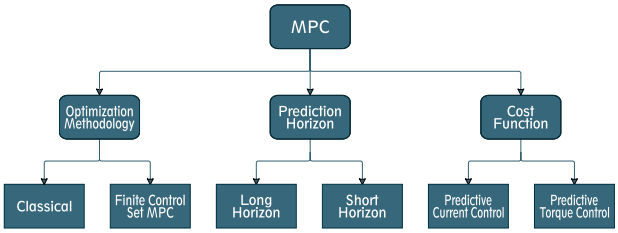

FIGURE 1. Classification of MPC.

Based on optimization methodology, in classical MPC, the result of optimization problem is the converter output voltage which later modified to get the required gating pulses, whereas in FCS-MPC [24], the discrete possible voltage vectors associated with the converter are tested in a cost function, and the minimum cost associated to a voltage vector is selected thereby giving the pulses directly. In terms of prediction horizon, long prediction horizon MPC predicts the future states for more than two steps i.e. $Np > 2$ (number of predictions) [25], while in short prediction horizon MPC, only the next future state is predicted. As far as classification based on cost function is concerned, there are many trends that have been reported in literature. Predictive current control (PCC) [24], [26]–[28] and Predictive torque control (PTC) [29]–[31] are the most general classification in terms of cost function. In PCC, cost function is composed of minimization of the error between stator currents, whereas in PTC, cost function evaluates minimum of the error in the torque and stator flux with respect of the reference values. Cost function can be augmented to include more goals like minimum switching frequency, suppressing certain harmonics, limiting the maximum value of motor parameters for protection purposes etc. [32].

Since the weighting factors of conventional FCS-MPTC depends also on the operating condition of the drive so designing these weighting factors for variable speed IM drive based on MPC is very challenging [33]. A lot of researchers have proposed different methods that incorporates weighting-factor calculations in the main MPC algorithm. Even to date there is no analytical method to find the optimal weighting factor for FCS-MPC. Mostly in literature the weighting factor is adjusted based on different iterative valuation methods [34].

The earliest method proposed in [35] to select the weighting factor was based on the rated stator flux and torque as a starting point and later tuned manual during the drive operation. In [36], analytical relationship for the weighting factors of FCS-MPC was formulated that shows the its dependence on the operating condition of the drive. Here the optimized weighting factor relation was determined in relation to changing torque and flux. It was observed during the actual MPC algorithm that the weighting factor updates its value each time the operating condition was changed. In [31] torque and stator flux reference values for FCS-MPTC was converted to flux equivalent vector that helps eliminates the need of weighting factor. In [29] another weighting factor elimination algorithm was proposed where the resultant solutions of cost function for each voltage vector is sorted & ranked. The VV with the highest rank is selected but the computational cost of this method grows exponentially with increasing switching states (voltage vectors) and the size of prediction horizon. Sugeno fuzzy method based online optimization of weighting factor for four switch two leg inverter fed IM was proposed in [37] but this work was only restricted to MATLAB simulation and no experimental validation was given. Particle swarm optimization based FCS-MPTC was proposed in [38] where the simple minimization of cost function was replaced with PSO in order to improve the steady state torque ripple. In [39], [40] optimized weighting factor was given in terms of rotor flux and reference voltage for matrix inverter fed IM. Here the author only studied the effect of weighting factor optimization for torque and ignore the switching losses in the inverter. Similarly, FCS-MPTC with online optimal weighting factor selection based on TOPSIS decision-making was studied in [41] based on the same performance criteria. In [42], author proposed an improved weighting factor elimination version of FCS-MPTC by creating a loop-up table of four vectors to be used with the cost function evaluation of FCS-MPTC technique. The proposed algorithm not only suggested the major improvement over the conventional FCS-MPTC technique but also considerably reduces the computational time owing to the fact that only four vectors are used instead of seven for MPTC cost function. To counter the torque ripple in steady-state or during load variation, A. Ammar et al. replaced the conventional PI modulator for external speed regulation loop with a fuzzy-logic controller [43]. The authors reported a reduction of torque ripple from 2 Nm to 0.5 Nm for the slow speed region. One other advantage of using the fuzzy logic controller was it drastically reduces the time of speed reversal also established experimentally in [43]. Lately, switching

variation associated with FCS-MPTC, due to the absence of any switching frequency modulator, was studied in [44]. The author proposed to use a mandatory zero vector with an active vector to be applied at the inverter alternatively for constant switching variation. Also, the computational time improvement was made because only active vectors were used with the cost function calculation. The one major disadvantage of their proposed algorithm is slow dynamic response to speed change because of switching a zero vector in every other sampling instant. F. Wang et al. in 2019 proposed their parallel predictive torque control (PPTC) algorithm for IM [45]. In PPTC, both torque and flux cost optimization were done simultaneously, and an adaptive mechanism was introduced to choose the optimal vector to switch at the inverter selected from three sorted arrays. Although the proposed method gives minor improvements over the torque and flux ripple in comparison to conventional FCS-MPTC, but the computational complexity of the algorithm makes it unrealizable to parametric variations.

The latest work on weighting factor optimization for FCS-MPTC was reported in [32] where the author applied the NSGA-II to find the Pareto optimal front for optimal weighting factors and evaluate each solution based on switching loss, total harmonic distortion, torque and flux ripple performance criteria. Here the only drawback was that author didn't consider the variable speed drive and no decision-making was made for the best compromised weighting factors.

Based on the above literature review and the latest reported work for FCS-MPTC with optimized weighting factors in [32], an improved algorithm with best compromised weighting factors obtained through the combination of NSGA-II with TOPSIS decision-making criteria is proposed. Average switching frequency reduction (ASFR) is implemented to eliminate the use of weighting factor for switching frequency term in the cost function. ASFR helps in the reduction of computationally time and somewhat avoids the intrinsic over current problem usually encounters with conventional MPTC. The proposed algorithm also caters the problem of peak rush current during the speed change by selecting zero vector as the optimal vector to be switched at the inverter whenever the predicted current exceeds the rated value of IM.

III. DISCRETE MODEL OF THREE PHASE INDUCTION MOTOR

Three phase induction motor dynamic model can be written in different forms depending on the selected frame of reference. In stator frame of reference, the stator and rotor voltage equations for the squirrel cage motor can be written as [34]

$$v_s^s = R_s^s i_s^s + p\psi_s^s \tag{1}$$

$$0 = R_r^s i_r^s + p\psi_r^s - j\omega_r^s \psi_r^s \tag{2}$$

here, the superscript is for frame of reference and the subscript is for stator and rotor quantities. Similarly, for the flux linkages

$$\psi_s^s = L_s^s i_s^s + L_m^s i_r^s \tag{3}$$

$$\psi_r^s = L_r^s i_r^s + L_m^s i_s^s \tag{4}$$

Choosing quadrature $(\alpha - \beta)$ stator currents and rotor flux as state vectors, the above dynamic model can be represented in state space form as

$$\dot{x}(t) = \mathbf{A}\left(\omega(t)\right) x(t) + \mathbf{B}u(t) \tag{5}$$

where, $x(t) = \left(i_s^\alpha \; i_s^\beta \; \psi_r^\alpha \; \psi_r^\beta\right)^T$ are state variables and $u(t) = \left(v_s^\alpha \; v_s^\beta\right)^T$ are the quadrature stator voltages. Here, also the above subscript shows the $(\alpha - \beta)$ stationary frame of reference and the below subscript represents the stator/rotor quantities. Matrices **A** and **B** are defined as

$$\mathbf{A} = \begin{bmatrix} -\frac{1}{\tau_s^s} & 0 & \frac{k_r^s}{R_\sigma \tau_s^s \tau_r^s} & \frac{k_r^s}{R_\sigma \tau_s^s \tau_r^s} \\ 0 & -\frac{1}{\tau_s^s} & -\frac{k_r^s}{R_\sigma \tau_s^s \omega_r^s} & \frac{k_r^s}{R_\sigma \tau_s^s \tau_r^s} \\ \frac{L_m^s}{\tau_r^s} & 0 & -\frac{1}{\tau_r^s} & -\omega_r^s \\ 0 & \frac{L_m^s}{\tau_r^s} & \omega_r^s & \frac{-1}{\tau_r^s} \end{bmatrix} \tag{6}$$

$$\mathbf{B} = \begin{bmatrix} \frac{1}{R_\sigma \tau_s^s} & 0 \\ 0 & \frac{1}{R_\sigma \tau_s^s} \\ 0 & 0 \\ 0 & 0 \end{bmatrix} \tag{7}$$

here, $k_r^s = \frac{L_m^s}{L_r^s}$ is the rotor coupling factor, $R_\sigma = R_s^s + k_r^{s2} R_r^s$ is the equivalent resistance, $\tau_s^s = \frac{L_\sigma}{R_\sigma}$ is the stator transient time constant, and $\tau_r^s = \frac{L_r^s}{R_r^s}$ is the rotor time constant.

The electromagnetic torque can be defined as

$$T = 1.5 n_p \left(\overrightarrow{\psi_s^s} \times \overrightarrow{i_s^s}\right) \tag{8}$$

where n_p is the number of pole pairs.

Since FCS-MPTC is a control algorithm that exploit the discrete nature of the intrinsic voltage vectors of SSTPI, it requires model of IM to be represented in discrete form. Using the Taylor series approximation, the discrete state space model of IM can be written as

$$x(k+1) = \mathbf{A}_d \omega(k) x(k) + \mathbf{B}_d u(k) \tag{9}$$

where, $\mathbf{A} = I + T_s \mathbf{A}$, $\mathbf{B}_d = T_s \mathbf{B}$ and T_s is the sampling time for MPC.

IV. THREE LEG SIX SWITCH INVERTER

The two-level voltage source inverter with three legs having two switches per leg is one of the most commonly used inverters with IM shown in Figure 2. It is also termed as six switch three phase inverter (SSTPI) or B6-inverter.

Because of six switches this inverter has eight distinct switching states that leads to six active and two zeros vectors. The space vector (SV) diagram of SSTPI is shown in Figure 3 where, vectors $(v_1 - v_6)$ are termed as active or voltage vectors whereas (v_0, v_7) are the two intrinsic zero or null vectors.

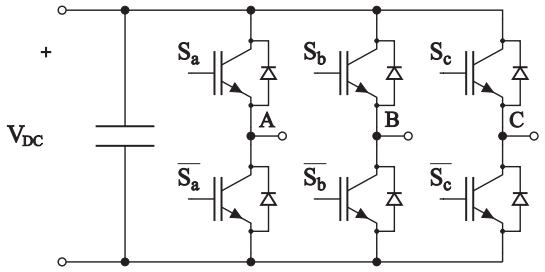

FIGURE 2. 2L-VSI with three legs.

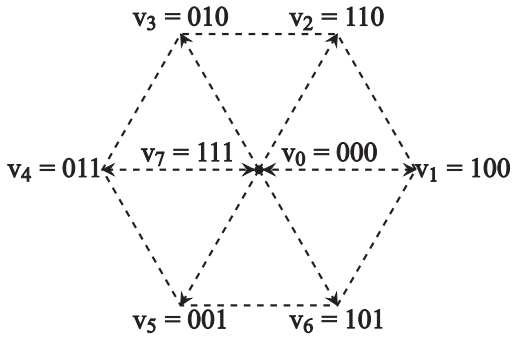

FIGURE 3. SV diagram of SSTPI.

Zero vectors do not contribute anything in terms of output voltage, but they are extremely important to minimize the switching loss of the inverter.

The input voltage applied by this inverter to IM, in stationary frame of reference, can be calculated as

$$u(t) = \mathbf{T}_c \times S_{abc}(t) \tag{10}$$

here, $S_{abc}(t)$ represents the switching state of the upper switches of each leg and $\mathbf{T}_c$ is the Clarke transformation matrix given as

$$\mathbf{T}_c = \frac{2}{3}\begin{bmatrix} 0 & -\frac{\sqrt{3}}{2} & \frac{\sqrt{3}}{2} \\ 1 & -\frac{1}{2} & \frac{1}{2} \end{bmatrix} \tag{11}$$

V. FINITE CONTROL SET MODEL PREDICTIVE TORQUE CONTROL OF INDUCTION MOTOR FED WITH SSTPI

The block diagram of FCS-MPTC of IM is shown in Figure 4. The workflow of this control technique is further explained below which is repeated for each control cycle.

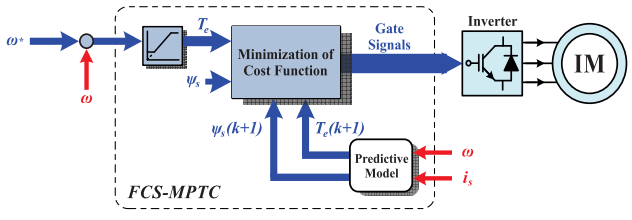

FIGURE 4. Block diagram of FCS-MPTC.

A. MEASUREMENT

The rotor speed along with stator stationary frame of reference currents are usually measured with external sensors as shown in Figure 4.

B. ESTIMATION

The estimation of stator flux can be done in either close loop or in open loop. Close loop observer with constant gain are more robust [37], but increases the computational cost of MPC overall. Stator flux can be estimated using open loop estimator with current and voltage equations of IM [29], [34]. Using the rotor dynamics, the rotor flux is estimated as

$$\widehat{\psi}_r^r = -\tau_r^s \frac{d\psi_r^r}{dt} + L_m^s \widehat{i}_s^r \tag{12}$$

It is to be noted that the inductance, resistance and rotor/stator time constants are independent of coordinate transformation.

Using the zero-order hold (ZOH), the discretized version of Eq. 12 can be expressed as

$$\widehat{\psi}_r^r(k) = e^{\frac{T_s}{\tau_r^s}} \widehat{\psi}_r^r(k-1) + L_m^s(1 - e^{\frac{T_s}{\tau_r^s}}) \widehat{i}_s^r(k-1) \tag{13}$$

The stator flux is then estimated at the 'k' interval as

$$\widehat{\psi}_s^r(k) = k_r^s \widehat{\psi}_r^r(k) + L_\sigma^s \widehat{i}_s^r(k) \tag{14}$$

Eqns. (12-14) are expressed in rotating frame of reference and a suitable coordination transformation (Park Transformation) is required to convert the quantities from rotating frame of reference to stationary frame of reference. It is usually done as follow

$$x^s = e^{j\theta_r} . x^r \tag{15}$$

where, x^s represents the stationary frame of reference quantity, x^r represents the rotating frame of reference quantity and θ_r represents the rotor position.

C. PREDICTION

Using Eq. (9) and Eqns. (14-15), stator flux and torque of induction motor are predicted for the '$k+1$' interval as

$$\widehat{\psi}_s^r(k+1) = k_r^s . \widehat{\psi}_r^r(k+1) + L_\sigma^s \widehat{i}_s^r(k) \tag{16}$$

$$\widehat{\psi}_s^s(k+1) = e^{j\theta_r} . \widehat{\psi}_s^r(k+1) \tag{17}$$

$$\widehat{T}(k+1) = 1.5 n_p \left(\overrightarrow{\widehat{\psi}_s^s(k+1)} \times \overrightarrow{i_s^s(k+1)} \right) \tag{18}$$

D. OPTIMIZATION

In FCS-MPTC a predefined cost function is used to evaluate the cost for all the possible intrinsic VVs shown in Figure 3. A voltage vector is selected which gives the minimum cost for the function value. The cost function associated with the conventional FCS-MPTC is

$$g_i = \sum_{h=0}^{N} \left| T_{ref}(k+h) - \widehat{T}(k+h) \right| + \lambda * \left| \psi_{ref}(k+h) - \widehat{\psi}_s^s(k+1) \right| \tag{19}$$

where, g_i is the cost for the 'i' voltage vector, 'h' represents the simulation step index and 'N' represents the total simulation steps. Instead of taking the quadratic error between the reference and predicted values, absolute error is used because of computational simplicity.

E. CONTROL LAW APPLICATION

The cost function defined in Eq. (19) makes a single objective optimization problem. 'λ' is the weighting factor used to give formal preference between the conflicting objective. The voltage vector corresponding to the minimum value of Eq. (19) is determined and applied for the next control period.

$$V_{opt} = arg \min_{\{v_0,\ldots,v_7\}} g_i \tag{20}$$

VI. STATOR FLUX WEIGHTING FACTOR OPTIMIZATION USING NON-DOMINATED SORTING GENETIC ALGORITHM-II

In conventional FCS-MPTC, only two objectives, error between the torque reference and estimated torque, and error between the stator flux reference and estimated stator flux, are used. However, the weighting factor used with the stator flux absolute error needs manual tuning for acceptable performance which is very cumbersome. Using heuristic optimization techniques this problem can be solved very effectively.

In this paper a cost function of the following form was used for FCS-MPTC

$$g_i = \sum_{h=0}^{N} \lambda_1 * \left|T_{ref}(k+h) - \widehat{T}(k+h)\right| + \lambda_2 * \left|\psi_{ref}(k+h) - \widehat{\psi}_s^s(k+1)\right| \tag{21}$$

here, λ_1, the weighting factor associated with the control of torque target value, can have value either positive or zero based on the desired torque error band whereas, λ_2, the weighting factor associated with flux error, is used for defining the preference between torque and flux error dynamics.

λ_1 can be defined as

$$\lambda_1 = \begin{cases} 0, & \text{if } \left|T_{ref}(k+h) - \widehat{T}(k+h)_i\right| \leq T_{band} \\ \lambda_T, & \text{if } \left|T_{ref}(k+h) - \widehat{T}(k+h)_i\right| > T_{band} \end{cases} \tag{22}$$

here, λ_T is chosen to be '1'. Similarly, for λ_2 the following relation is used

$$\lambda_2 = \lambda_\psi \frac{T_{norm}}{|\psi_{norm}|} \tag{23}$$

where, 'T_{norm}' and 'ψ_{norm}' are the nominal values of IM.

A. NON-DOMINATED SORTING GENETIC ALGORITHM-II

The weighting factors in conventional MPTC technique effects the drive performance. Also, the cost function for MPTC usually has two conflicting objectives to be optimized, a global multi-objective algorithm can provide set of the best solutions rather than a single solution obtained using traditional multi-objective solving methods like weighting method and ε-constraint method, known as the Pareto solutions or non-dominated solutions. The basic features of any multi-objective global optimization are:

- Search for Pareto front (convergence)
- Maintain the diversity in solutions for next generations to cover the whole range of optimal possibilities (diversity)

NSGA-II is a global multi objective optimization algorithm proposed, as an improvement over NSGA-I algorithm, by Deb et al. in 2002. By introducing the elite strategy based on the crowding distance and rank operator of fast non-dominated sorting algorithm, the computational complexity of the algorithm is reduced. The other difference between NSGA-I and NSGA-II is the diversity in chromosome population. Compared with traditional multi-objective solving methods, such as weighting method and ε-constraint method, this method is not affected by proper constraint limit settings, target weights, etc.

Each individual solution in NSGA-II contains the value of parameters to be simultaneously optimized. The pseudo code for NSGA-II is shown in Algorithm 1.

Algorithm 1 Pseudo Code for NSGA-II

```
Initialize random population N of dimensions size equal to parameter size in the search space
while Termination condition not reached do
  for Each individual solution x_i do
    Perform genetic operations (crossover & mutation)
    Evaluate fitness of all x_i's in population
    Rank all x_i's based on dominance
    Calculate crowding distance for every x_i
    if Rank of x_i ≥ x_j then
      Select x_i
    end if
    while Population size < N do
      Select x_i's based on crowding distance
    end while
  end for
end while
```

It is to be noted that the multi-objective evolutionary optimization algorithms returns a specific number of solutions called the Pareto solutions. To get the best compromised solution, a decision making method is usually used after the optimization to get the best solution out of all the solutions in Pareto front.

B. TOPSIS FOR BEST COMPROMISED SOLUTION

Technique for order preference by similarity to an ideal solution (TOPSIS) is a relatively easy decision-making method proposed in [46] and is based on combining functions that determines the relevance of a solution to an ideal solution. The idea is to select a compromised solution out of a Pareto front whose distance is smallest from the idea solution and

greatest to the complement of the ideal solution. The pseudo code for TOPSIS is given in Algorithm 2.

Algorithm 2 Pseudo Code for TOPSIS

1: Calculate the normalized decision matrix
2: Evaluate the weighted normalized decision matrix
3: Evaluate fitness of all x_i's in population
4: Find ideal and compliment of ideal solution
5: Calculate the separation distance matrix for each solution
6: Measure the relative closeness of each solution to ideal solution
7: Rank the solutions
8: Pick the 1^st one.

C. FCS-MPTC OPTIMIZATION WITH NSGA-II

To get the optimized torque and flux weighting factors, each individual chromosome of NSGA-II (possible solution) has two genes as given below.

$$x_i = \left[T_{band} \lambda_\psi\right] \tag{24}$$

1) 'T_{band}', whose values are set between the 5% to 15% of the nominal torque value of IM.
2) 'λ_ψ', whose value was restricted between 1 to 20.

A step speed of 30% of rated value and 75% of the rated torque is applied during the MATLAB/Simulink simulation for the evaluation of each possible solution. Steady-state flux and torque ripples (T_{rip}, ψ_{rip}) were extracted from the simulation and a fitness function was defined based on combined error between the flux and torque ripple. A Pareto front with best compromised solution based on TOPSIS decision method is shown in Figure 5.

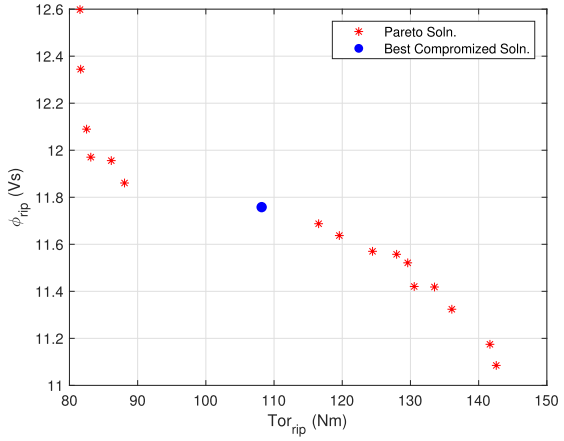

FIGURE 5. Pareto front with best compromised solution.

Since, the NSGA-II is a heuristic technique greatly affected by the randomness introduced in the solution population, this process was repeated 5 times and an average of the best compromised solutions obtained, after the TOPSIS based decision making, was chosen for experimental verification.

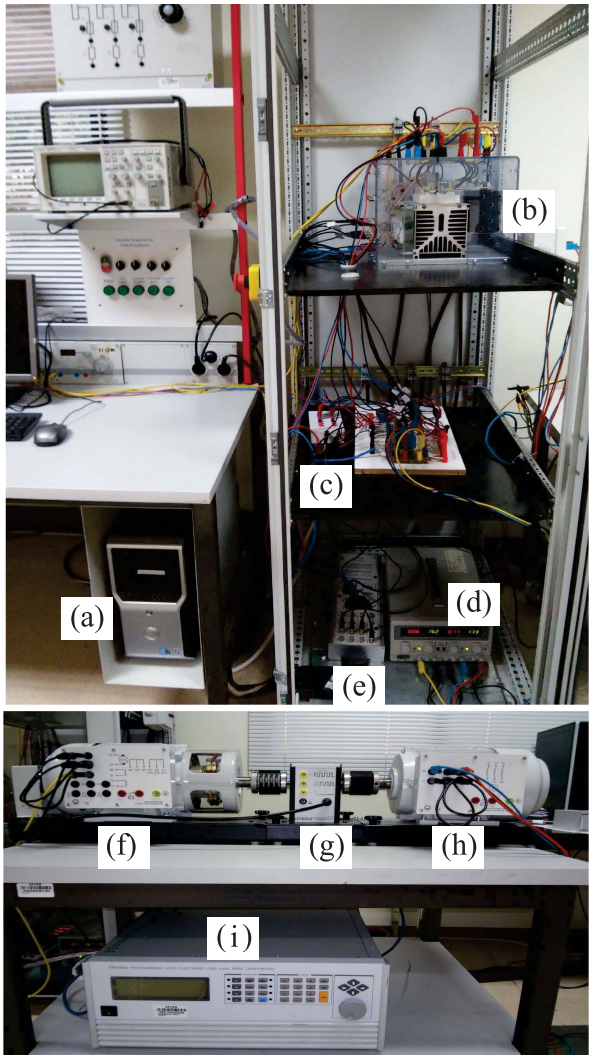

FIGURE 6. Experimental Setup *(a) Host Computer (b) Industrial Inverter (c) Current Sensors (d) ± 15V DC Power Supply (e) dSPACE Interference Terminal Box (f) DC Generator (g) Speed Encoder (h) Induction motor (i) Programmable Load.*

TABLE 1. Parameters of 3-Φ induction motor.

Parameter	Value	Unit
ω_{norm}	1710	rpm
T_{norm}	5.5	Nm
ψ_{norm}	0.8157	Wb
R_s	8.15	Ω
R_r	6.0373	Ω
L_s	0.4577	H
L_r	0.4577	H
L_m	0.4372	H
n_p	2	
J	0.07	Kg.m^2
B	0	N/rad/s

VII. EXPERIMENTAL RESULTS

MATLAB r2019b was used to first find the optimized weighting factors of the cost function given in Eq. 21. The parameters for IM and NSGA-II used are tabulated in Table 1-2.

TABLE 2. Parameters of NSGA-II.

Parameter	Type	Value
Population Size	Randomly Initiated	50
Selection	Tournament	2
Crossover	Blx - α	0.5
Mutation	Nonuniform	–
Stopping Criteria	Max. # of Generations	100

TABLE 3. Average optimal solution from five runs of NSGA-II.

Parameter	Type	Value
T_{band}	Torque Ripple Band	0.30822
λ_ψ	Flux Weighting Factor	3.5906

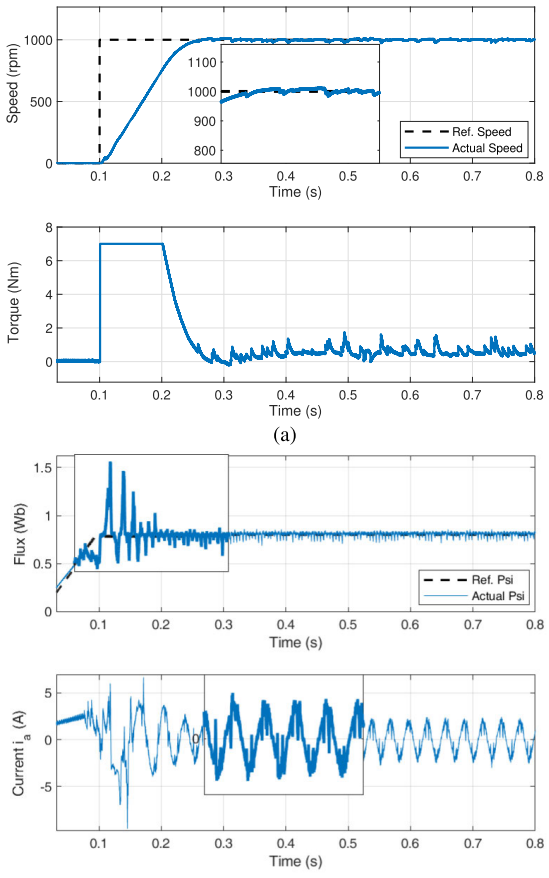

FIGURE 7. Measure response from Conventional FCS-MPTC drive without Optimized Weighting Factor at no load: *(a) Reference and output speed comparison, Electromagnetic Torque response (b) Reference and actual stator flux comparison, Input phase A current.*

A simple PI controller was used for speed tracking with $K_p = 21$ and $K_i = 2$. FCS-MPTC sampling rate was fixed at 20 kHz which was same as the sampling frequency for the entire model. Speed control loop sampling rate was set to 10 kHz. The average optimized solution obtained after applying the TOPSIS method to the Pareto front secured from the five different runs of NSGA-II for T_{band} and λ_ψ are shown in Table 3.

To examine the performance of proposed algorithm, the dynamics response of the motor was measured using

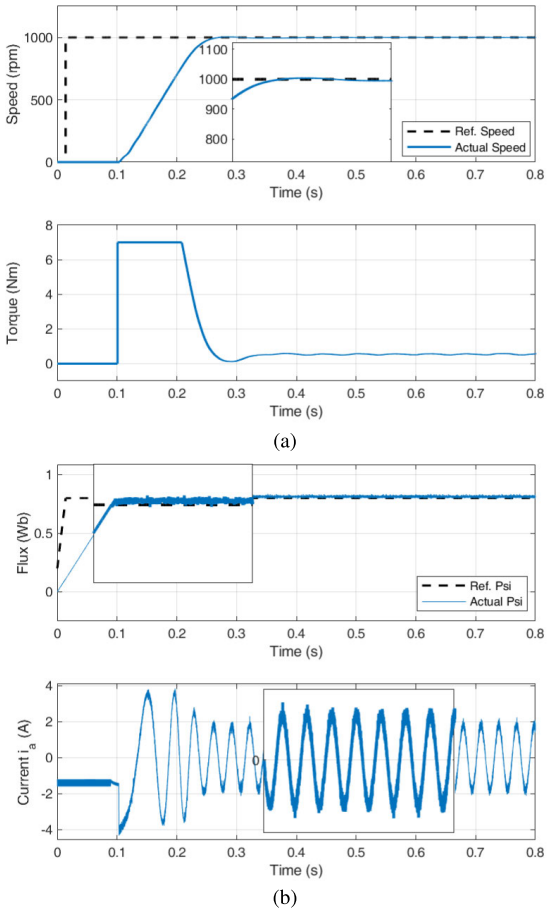

FIGURE 8. Measure response from Conventional FCS-MPTC drive with Optimized Weighting Factor at no load: *(a) Reference and output speed comparison, Electromagnetic Torque response (b) Reference and actual stator flux comparison, Input phase A current.*

the experimental setup shown in Figure 6. The experimental results for the FCS-MPTC with conventional values of weighting factors i.e. ($\lambda_1 = 1, \lambda_\psi = 1$) corresponding to '$\lambda_2$' given by Eq. 22, and with optimized weighting factors (given in Table 3) were obtained at no load, and with a load of 3.5 Nm.

A. AT NO LOAD

First the IM was given an initial flux setup command just to minimize the startup torque ripple. Then, a step speed command of 1000 rpm was given at 0.1s. Figure 7-8 shows the measure response of conventional and optimized FCS-MPTC respectively.

From the visual inspection of Figure 7-8, it can be easily seen that the proposed optimized technique outperforms the conventional FCS-MPTC algorithm.

B. WITH LOAD

Chroma programmable load was used in constant current mode with DC generator to load the IM. A load command of 3.5 Nm was applied at 0.8s. The measure response for both conventional and optimized FCS-MPTC are shown in Figure 9-10.

TABLE 4. Performance indices of conventional FCS-MPTC and proposed FCS-MPTC (experimental results).

	Type	$\mathbf{T_{rip}}\%$	$\psi_{\mathbf{rip}}\%$	$\mathbf{I_{thd}}\%$	$\mathbf{f_{av}(KHz)}$
At No Load	Conventional	15.77	5.97	6.32	6.45
	Optimized	1.43	2.78	5.13	6.40
With Load	Conventional	6.23	5.25	6.18	6.29
	Optimized	1.42	2.57	5.12	6.25

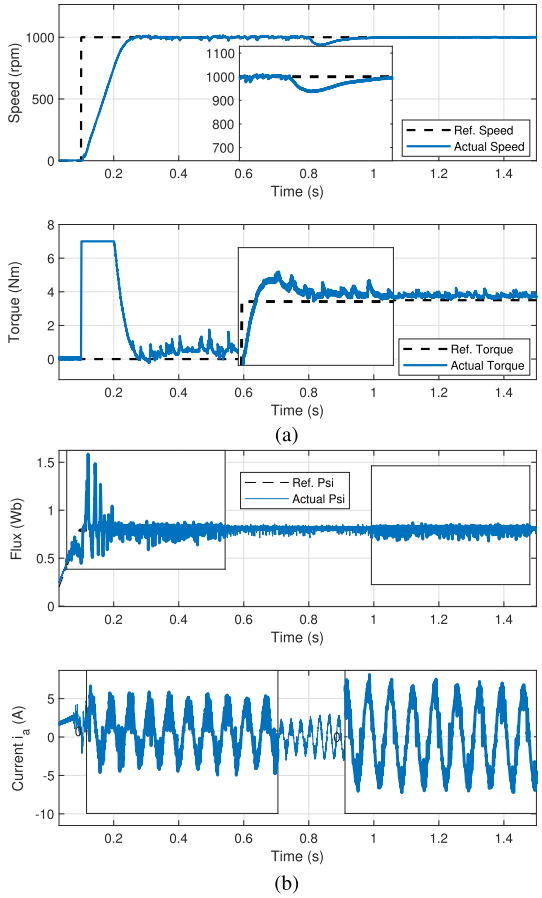

FIGURE 9. Measure response from Conventional FCS-MPTC drive without Optimized Weighting Factor with 3.5Nm load: *(a) Reference and output speed comparison, Electromagnetic Torque response (b) Reference and actual stator flux comparison, Input phase A current.*

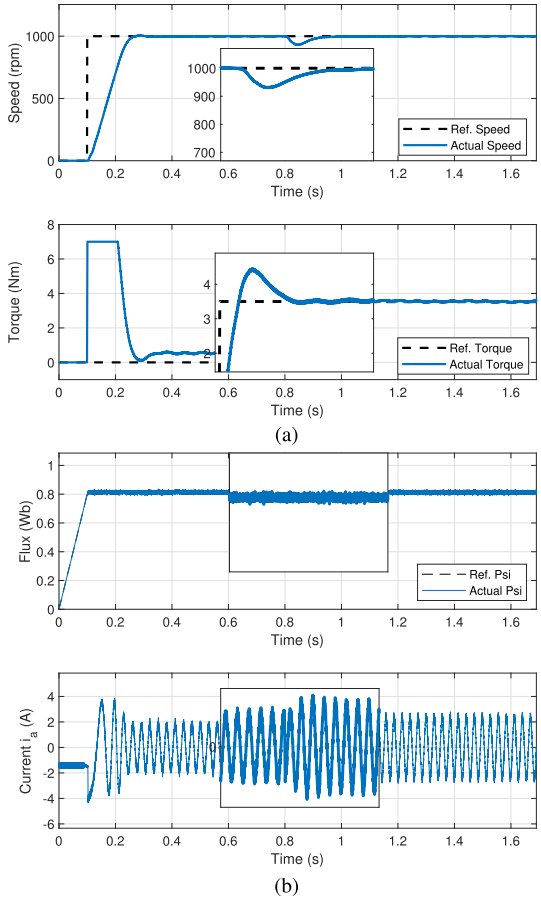

FIGURE 10. Measure response from Optimized FCS-MPTC drive without Optimized Weighting Factor with 3.5Nm load: *(a) Reference and output speed comparison, Electromagnetic Torque response (b) Reference and actual stator flux comparison, Input phase A current.*

The dynamic response of IM with optimized MPTC shows a torque ripple of 1.43% in contrast to 6.23% with conventional MPTC. Also, the input phase current is very sinusoidal in case of optimized MPTC.

VIII. DISCUSSION

Table 4 quantifies the performance of optimized FCS-MPTC in comparison to conventional FCS-MPTC based on torque ripple per rated torque, flux ripple per rated flux, THD of the input phase current, and the average switching frequency performance indices.

The results obtained justifies the fact that proposed scheme with optimized weighting factor best compromises the performance to ripple measurement for both torque and flux, further vindicating the usefulness of NSGA-II with TOPSIS decision making criteria (for best compromised solution) for the optimization of FCS-MPTC weighting factors.

Also, the speed tracking in case of proposed FCS-MPTC only changes significantly during the load change while in case of conventional FCS-MPTC, although the IM is tracking the reference speed of 1000 rpm but the zoomed image in both case (no load & with load) shows abrupt variations.

The optimal frequency control does show satisfactory improvement in the switching frequency, but this can be further improved by incorporating a new term in the cost function of FCS-MPTC related to the switching frequency. However, this will also increase the computational cost of the algorithm and a delay compensation will become necessary.

Also, it is to be noted that a protection against the over-current was also implemented with the term I_m in the cost function of studied FCS-MPTC. The reason for over-current protection was to avoid switching a voltage vector that might causes the IM input current to exceed the rated value. In case of such an event, zero voltage vector

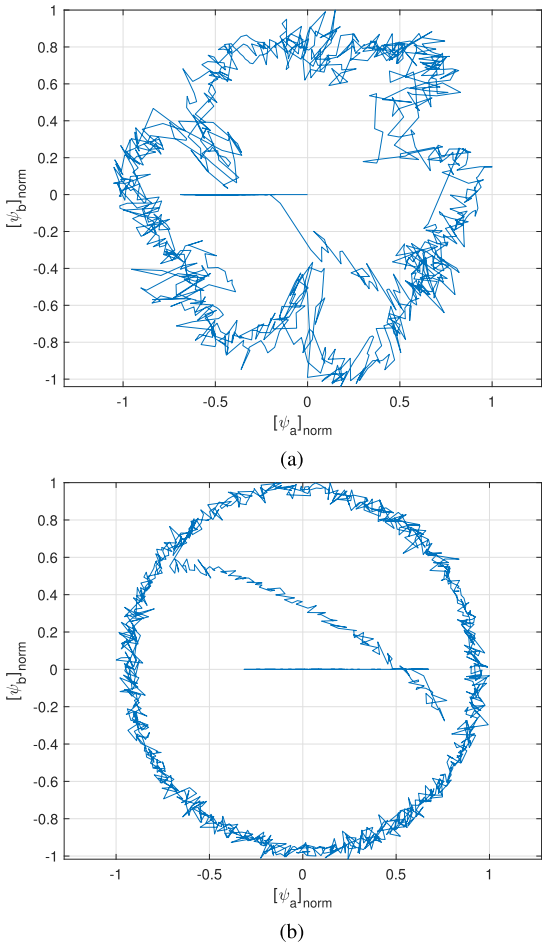

FIGURE 11. Steady-state normalized Stator Flux Trajectory: *(a) Stator Flux Trajectory for conventional FCS-MPTC (b) Stator Flux Trajectory for optimized FCS-MPTC.*

was switched disregarding the optimal switching vector being obtained from the prediction block.

Figure 11 shows the normalized space vector trajectory for stator flux. Because of optimal switching frequency control, the flux space vector rotates in a circular fashion for the proposed technique further verifying the improved THD values for the input phase current shown in Table 4. The space vector trajectory for conventional FCS-MPTC shows major variations especially at the start of each rotating cycle for the space vector.

IX. CONCLUSION

A speed control IM drive based on FCS-MPTC technique was studied. The weighting factors in the conventional FCS-MPTC cost function was optimized based on certain constraints using NSGA-II with TOPSIS decision making criteria. An experimental validation of the proposed method was carried out. The THD value for the phase current shows remarkable improvement over the conventional method under no load condition. The percentage change in torque and flux ripple is very negligible under no load and with load conditions showing the robustness of the proposed technique. Although, the peak current control was implemented for both conventional and optimized case during the experimental evaluation for the protection of IM, the proposed algorithm reduces the input phase current value by about 20%. The ASFR control does reduce the switching losses but it greatly improves the SV trajectory of the rotating stator flux which thereby improves the THD of stator current. This approach can be further extended to any FCS-MPC strategy requiring the design of weighting factors. Future aspects of this research will be to use the proposed methodology for multilevel inverter-based IM drive in accordance with constraints to balance out the capacitor bank voltage.

REFERENCES

[1] P. Vas, *Sensorless Vector and Direct Torque Control*. Oxford, U.K.: Oxford Univ. Press, 1998.
[2] A. Emadi, *Advanced Electric Drive Vehicles*. Boca Raton, FL, USA: CRC Press, 2014.
[3] M. Olszewski, "Annual progress report for the power electronics and electric machinery program," United States Dept. Energy, Oak Ridge Nat. Lab., Oak Ridge, TN, USA, 2005, p. 182.
[4] A. Vagati, G. Pellegrino, and P. Guglielmi, "Comparison between SPM and IPM motor drives for EV application," in *Proc. IEEE 19th Int. Conf. Elect. Mach. (ICEM)*, Sep. 2010, pp. 1–6.
[5] M. Liserre, R. Cardenas, M. Molinas, and J. Rodriguez, "Overview of multi-MW wind turbines and wind parks," *IEEE Trans. Ind. Electron.*, vol. 58, no. 4, pp. 1081–1095, Apr. 2011.
[6] B. K. Bose, *Power Electronics and AC Drives*. Upper Saddle River, NJ, USA: Prentice-Hall, 1986.
[7] D. W. Novotny and T. A. Lipo, *Vector Control and Dynamics of AC Drives*, vol. 41. Oxford, U.K.: Oxford Univ. Press, 1996.
[8] M. Depenbrock, "Direct self-control (DSC) of inverter fed induktion machine," in *Proc. IEEE Power Electron. Spec. Conf.*, Jun. 1987, pp. 632–641.
[9] I. Takahashi and Y. Ohmori, "High-performance direct torque control of an induction motor," *IEEE Trans. Ind. Appl.*, vol. 25, no. 2, pp. 257–264, Mar. 1989.
[10] P. Tiitinen and M. Surandra, "The next generation motor control method, DTC direct torque control," in *Proc. IEEE Int. Conf. Power Electron., Drives Energy Syst. Ind. Growth*, vol. 1, Jan. 1996, pp. 37–43.
[11] H. Le-Huy, "Comparison of field-oriented control and direct torque control for induction motor drives," in *Proc. IEEE 34th IAS Annu. Meeting. Conf. Rec. Ind. Appl. Conf.*, vol. 2, Oct. 1999, pp. 1245–1252.
[12] G. S. Buja and M. P. Kazmierkowski, "Direct torque control of PWM inverter-fed AC motors-A survey," *IEEE Trans. Ind. Electron.*, vol. 51, no. 4, pp. 744–757, Aug. 2004.
[13] Y.-S. Lai and J.-H. Chen, "A new approach to direct torque control of induction motor drives for constant inverter switching frequency and torque ripple reduction," *IEEE Trans. Energy Convers.*, vol. 16, no. 3, pp. 220–227, Sep. 2001.
[14] T. G. Habetler, F. Profumo, M. Pastorelli, and L. M. Tolbert, "Direct torque control of induction machines using space vector modulation," *IEEE Trans. Ind. Appl.*, vol. 28, no. 5, pp. 1045–1053, Sep. 1992.
[15] H. Abu-Rub, M. R. Khan, A. Iqbal, and S. M. Ahmed, "MRAS-based sensorless control of a five-phase induction motor drive with a predictive adaptive model," in *Proc. IEEE Int. Symp. Ind. Electron. (ISIE)*, Jul. 2010, pp. 3089–3094.
[16] T. Orlowska-Kowalska and M. Dybkowski, "Stator-current-based MRAS estimator for a wide range speed-sensorless induction-motor drive," *IEEE Trans. Ind. Electron.*, vol. 57, no. 4, pp. 1296–1308, Apr. 2010.
[17] S. A. Davari, D. A. Khaburi, F. Wang, and R. Kennel, "Using full order and reduced order observers for robust sensorless predictive torque control of induction motors," *IEEE Trans. Power Electron.*, vol. 27, no. 7, pp. 3424–3433, Jul. 2011.
[18] J. H. Lee, "Model predictive control: Review of the three decades of development," *Int. J. Control, Autom. Syst.*, vol. 9, no. 3, p. 415, Jun. 2011.
[19] C. E. Garcia, D. M. Prett, and M. Morari, "Model predictive control: Theory and practice—A survey," *Automatica*, vol. 25, no. 3, pp. 335–348, 1989.

[20] S. Vazquez, J. I. Leon, L. G. Franquelo, J. Rodriguez, H. A. Young, A. Marquez, and P. Zanchetta, "Model predictive control: A review of its applications in power electronics," *IEEE Ind. Electron. Mag.*, vol. 8, no. 1, pp. 16–31, Mar. 2014.
[21] J. Rodriguez, M. P. Kazmierkowski, J. R. Espinoza, P. Zanchetta, H. Abu-Rub, H. A. Young, and C. A. Rojas, "State of the art of finite control set model predictive control in power electronics," *IEEE Trans. Ind. Informat.*, vol. 9, no. 2, pp. 1003–1016, May 2013.
[22] F. Wang, X. Mei, J. Rodriguez, and R. Kennel, "Model predictive control for electrical drive systems-an overview," *CES Trans. Elect. Mach. Syst.*, vol. 1, no. 3, pp. 219–230, Sep. 2017.
[23] S. Vazquez, J. Rodriguez, M. Rivera, L. G. Franquelo, and M. Norambuena, "Model predictive control for power converters and drives: Advances and trends," *IEEE Trans. Ind. Electron.*, vol. 64, no. 2, pp. 935–947, Feb. 2017.
[24] J. Rodriguez, J. Pontt, C. A. Silva, P. Correa, P. Lezana, P. Cortés, and U. Ammann, "Predictive current control of a voltage source inverter," *IEEE Trans. Ind. Electron.*, vol. 54, no. 1, pp. 495–503, Feb. 2007.
[25] T. Geyer, G. Papafotiou, and M. Morari, "Model predictive direct torque control—Part I: Concept, algorithm, and analysis," *IEEE Trans. Ind. Electron.*, vol. 56, no. 6, pp. 1894–1905, Jun. 2009.
[26] J. C. R. Martinez, R. M. Kennel, and T. Geyer, "Model predictive direct current control," in *Proc. IEEE Int. Conf. Ind. Technol. (ICIT)*, Mar. 2010, pp. 1808–1813.
[27] J.-M. Rétif, X. Lin-Shi, and F. Morel, "Predictive current control for an induction motor," in *Proc. IEEE Power Electron. Spec. Conf. (PESC)*, Jun. 2008, pp. 3463–3468.
[28] D. G. Holmes and D. A. Martin, "Implementation of a direct digital predictive current controller for single and three phase voltage source inverters," in *Proc. IEEE 31st IAS Annu. Meeting Ind. Appl. Conf. (IAS)*, vol. 2, Oct. 1996, pp. 906–913.
[29] C. A. Rojas, J. Rodríguez, F. Villarroel, J. R. Espinoza, C. A. Silva, and M. Trincado, "Predictive torque and flux control without weighting factors," *IEEE Trans. Ind. Electron.*, vol. 60, no. 2, pp. 681–690, Feb. 2012.
[30] C. A. Rojas, S. Kouro, M. Perez, and F. Villarroel, "Multiobjective fuzzy predictive torque control of an induction machine fed by a 3L-NPC inverter," in *Proc. IEEE Int. Symp. Predictive Control Electr. Drives Power Electron. (PRECEDE)*, Oct. 2015, pp. 21–26.
[31] Y. Zhang and H. Yang, "Two-vector-based model predictive torque control without weighting factors for induction motor drives," *IEEE Trans. Power Electron.*, vol. 31, no. 2, pp. 1381–1390, Feb. 2016.
[32] P. R. U. Guazzelli, W. C. de Andrade Pereira, C. M. R. Oliveira, A. G. Castro, and M. L. Aguiar, "Weighting factors optimization of predictive torque control of induction motor by multiobjective genetic algorithm," *IEEE Trans. Power Electron.*, vol. 34, no. 7, pp. 6628–6638, Jul. 2019.
[33] M. Mamdouh, M. Abido, and Z. Hamouz, "Weighting factor selection techniques for predictive torque control of induction motor drives: A comparison study," *Arabian J. Sci. Eng.*, vol. 43, no. 2, pp. 433–445, 2018.
[34] P. Cortés, S. Kouro, B. L. Rocca, R. Vargas, J. Rodríguez, J. I. L. Galván, S. V. Pérez, and L. G. Franquelo, "Guidelines for weighting factors design in model predictive control of power converters and drives," in *Proc. IEEE Int. Conf. Ind. Technol. (ICIT)*, Gippsland, VIC, Australia, Feb. 2009, pp. 1–7.
[35] J. Rodriguez, R. M. Kennel, J. R. Espinoza, M. Trincado, C. A. Silva, and C. A. Rojas, "High-performance control strategies for electrical drives: An experimental assessment," *IEEE Trans. Ind. Electron.*, vol. 59, no. 2, pp. 812–820, Feb. 2012.
[36] S. A. Davari, D. A. Khaburi, and R. Kennel, "An Improved FCS–MPC algorithm for an induction motor with an imposed optimized weighting factor," *IEEE Trans. Power Electron.*, vol. 27, no. 3, pp. 1540–1551, Mar. 2012.
[37] D. Zhou, J. Zhao, and Y. Liu, "Online tuning of weighting factors based on sugeno fuzzy method in predictive torque control of four-switch three-phase inverter-fed IM," in *Proc. IEEE Int. Symp. Power Electron., Elect. Drives, Autom. Motion (SPEEDAM)*, Jun. 2016, pp. 734–739.
[38] T.-J. Su, T.-Y. Tsou, S.-M. Wang, T.-Y. Li, and H.-Q. Vu, "Torque ripple reduction of induction motor based on a hybrid method of model predictive torque control and particle swarm optimization," *Adv. Mech. Eng.*, vol. 8, no. 10, 2016, Art. no. 1687814016676465.
[39] M. Uddin, S. Mekhilef, M. Mubin, and M. Rivera "Model predictive torque ripple reduction with weighting factor optimization fed by an indirect matrix converter," *Electr. Power Compon. Syst.*, vol. 42, no. 10, pp. 1059–1069, 2014.
[40] M. Uddin, S. Mekhilef, M. Rivera, and J. Rodriguez, "Imposed weighting factor optimization method for torque ripple reduction of IM fed by indirect matrix converter with predictive control algorithm," *J. Electr. Eng. Technol.*, vol. 10, no. 1, pp. 227–242, 2015.
[41] V. P. Muddineni, S. R. Sandepudi, and A. K. Bonala, "Finite control set predictive torque control for induction motor drive with simplified weighting factor selection using TOPSIS method," *IET Electr. Power Appl.*, vol. 11, no. 5, pp. 749–760, 2017.
[42] M. Mamdouh and M. A. Abido, "Efficient predictive torque control for induction motor drive," *IEEE Trans. Ind. Electron.*, vol. 66, no. 9, pp. 6757–6767, Sep. 2019.
[43] A. Ammar, B. Talbi, T. Ameid, Y. Azzoug, and A. Kerrache, "Predictive direct torque control with reduced ripples for induction motor drive based on T-S fuzzy speed controller," *Asian J. Control*, vol. 21, no. 4, pp. 2155–2166, 2019. [Online]. Available: https://onlinelibrary.wiley.com/doi/abs/10.1002/asjc.2148
[44] S. Azadi, S. A. Davari, A. A. Ashtiani, C. Garcia, and J. Rodrigues, "Reducing variation of switching frequency in finite-state predictive torque of three-phase induction motor," in *Proc. IEEE 10th Int. Power Electron., Drive Syst. Technol. Conf. (PEDSTC)*, Feb. 2019, pp. 108–113.
[45] F. Wang, H. Xie, Q. Chen, S. A. Davari, J. Rodriguez, and R. Kennel, "Parallel predictive torque control for induction machines without weighting factors," *IEEE Trans. Power Electron.*, vol. 35, no. 2, pp. 1779–1788, Feb. 2020.
[46] C.-L. Hwang and K. Yoon, *Methods for Multiple Attribute Decision Making*. Berlin, Germany: Springer, 1981, pp. 58–191.

M. H. ARSHAD received the B.Sc. degree in electrical engineering from the University of the Punjab, Lahore, Pakistan. He is currently enrolled as a full-time Graduate Scholar with a major in control engineering with the Electrical Engineering Department, King Fahd University of Petroleum and Minerals, Dhahran, Saudi Arabia. His research focus is on power electronics, nonlinear dynamical systems, variable speed drives for multiphase induction motor, digital filter design, and flatness based robust control of nonlinear systems.

M. A. ABIDO (SM'15) received the B.Sc. (Hons.) and M.Sc. degrees in electrical engineering from Menoufia University, Shebeen El-Kom, Egypt, in 1985 and 1989, respectively, and the Ph.D. degree from the King Fahd University of Petroleum and Minerals (KFUPM), Dhahran, Saudi Arabia, in 1997. He is currently a Distinguished University Professor with KFUPM and a Senior Researcher with the K.A.CARE Energy Research and Innovation Center, Dhahran. His research interests are power system stability, planning, operation, and optimization techniques applied to power systems. He has published two books and more than 350 articles in reputable journals and international conferences. He participated in over 50 funded projects and supervised over 50 M.S. and Ph.D. students. He was a recipient of the KFUPM Excellence in Research Award in 2002, 2007 and 2012, the KFUPM Best Project Award in 2007 and 2010, the First Prize Paper Award of the Industrial Automation and Control Committee of the IEEE Industry Applications Society in 2003, the Abdel-Hamid Shoman Prize for Young Arab Researchers in Engineering Sciences in 2005, the Best Applied Research Award of the 15th GCC-CIGRE Conference, Abu Dhabi, United Arab Emirates, in 2006, and the Best Poster Award from the International Conference on Renewable Energies and Power Quality (ICREPQ'13), Bilbao, Spain, in 2013. He has been awarded the Almarai Prize for Scientific Innovation (2017–2018), as a Distinguished Scientist, Saudi Arabia, in 2018, and the Khalifa Award for Higher Education (2017–2018), as a Distinguished University Professor in Scientific Research, Abu Dhabi, in 2018.

ABOUBAKR SALEM received the B.Sc. and M.Sc. degrees in electrical engineering from Helwan University, Egypt, in 2004 and 2009, respectively, and the Ph.D. degree from Ghent University, Belgium, in 2015. He is currently a Visiting Assistant Professor with the Electrical Engineering Department, King Fahd University of Petroleum and Minerals (KFUPM). He is involved in several funded projects from KFUPM as Pi and Co-I. He has participated as a Co-I in funded projects from European Union (i.e., STS-Med and Euro-Sun-Med) with a fund of € 20 million. His research interests include power electronic converters design and control, electrical drives applications, renewable energy integration, electrical vehicles, and smart grid applications.

ABUBAKR H. ELSAYED received the B.S. degree in electrical engineering from King Fahd University of Petroleum and Minerals (KFUPM), Dhahran, Saudi Arabia, in 2016, where he is currently pursuing the M.Sc. degree in electrical engineering with a focus on power engineering as a full-time Graduate Student. His research interests include renewable energy integration, power electronics, electrical machine control, and sensorless control of electrical motors.